ELSEVIER

Theoretical and Applied Fracture Mechanics 28 (1997) 141–146

theoretical and applied fracture mechanics

Plastic deformation behavior of mild steel subjected to ultrasonic treatment

P.V. Makarov *, V.A. Romanova, R.R. Balokhonov

Institute of Strength Physics and Materials Science, Siberian Branch of Russian Academy of Sciences, 634021 Tomsk, Russia

Abstract

Investigated in this work is the plastic deformation of mild steel subjected to ultrasonic treatment. Such behavior could arise in machining where ultrasonic vibrations are introduced directly by ultrasonic concentrator and/or magnetic-strictive converter. An ultrasonic shock wave could also result. Calculated are the stress–time history and the tool displacement in addition to the accumulation of plastic deformation that reflects the material damage evolution process at the different scale levels. © 1997 Published by Elsevier Science Ltd.

1. Introduction

It is well known that steel tends to harden when deformed plastically as a result of damage evolution at the different scale levels that could lead to final fracture. Such a process prevails when metal specimens are subjected to ultrasonic loading. A mathematical model of plane wave propagation will be developed to describe the material response under both ultrasonic vibrations and shock waves. Numerical results are obtained and discussed in relation to the cold working of metal and possible damage by fracture of the surface layer.

2. Mathematical model

The one-dimensional plane wave propagation equation can be expressed in the form [1]

$$\rho\frac{\partial U_1}{\partial t}=\frac{\partial \sigma_1}{\partial x}. \tag{1}$$

The total strain rate is given by

$$\dot{\varepsilon}_1^{\mathrm{T}}=\frac{\partial U_1}{\partial x}=\frac{\partial V}{\partial t}, \tag{2}$$

in which the specific volume is $V=\rho_0/\rho$ with ρ_0 and ρ as initial and current density, respectively. In Eqs. (1) and (2), U_1 is the particle velocity and x the Langrangian coordinate. The constitutive equation is

$$\sigma_i=-P(\rho, E)+S_i, \tag{3}$$

where P is the average pressure, S_i the stress deviator, and E the internal energy.

Since the stresses induced by ultrasonics are small, the baro-tropic cubic expression may be used to describe the pressure,

$$P=A\Theta+B\Theta^2+C\Theta^3, \tag{4}$$

where Θ is the cubic strain. The coefficients A, B and C are defined in Refs. [2,3] for a number of materials.

The deviatoric stress is of the relaxation type,

$$\dot{S}_1=4\mu\left(\dot{\varepsilon}_1^{\mathrm{T}}-2\dot{\gamma}^{\mathrm{P}}\right)/3, \tag{5}$$

* Corresponding author.

0167-8442/97/$17.00
PII S0167-8442(97)00039-6

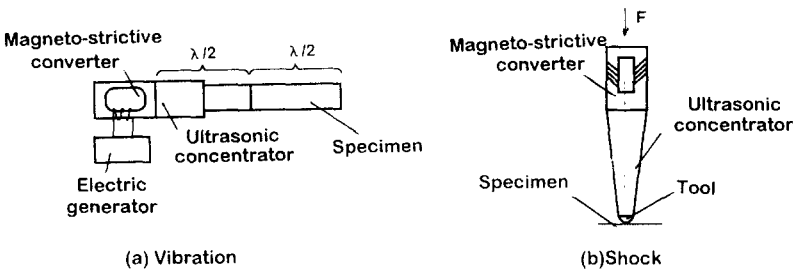

Fig. 1. Schematics of ultrasonic treatment: (a) vibration and (b) shock.

where μ is the shear modules. The plastic shear rate is $\dot{\gamma}^{p}$.

2.1. Plastic deformation

Plastic flow on micro-level is caused by the evolution of dislocation. In contrast to the conventional treatment that leaves out the plastic deformation at $\sigma < \sigma_{0.2}$, the present model assumes that any small disturbances could induce small plastic deformations. This approach has a great importance for ultrasonic loading, because the influence of a series of high frequency pulses (even at stresses below yield) can lead to considerable accumulation of high plastic deformation.

Total plastic deformation at each time-step of loading can be expressed as the sum of individual contributions from each dislocation fraction, i.e.,

$$\dot{\gamma}^{p} = \sum_{i} \Delta\dot{\gamma}_{i}^{p}, \qquad \Delta\dot{\gamma}_{i}^{p} = gbNfP_{i}(\tau_{si})\,v_{i}, \tag{6}$$

where $g = 0.5$ is the orientation factor, b the Burgers vector, N and f the dislocation density and the portion of movable dislocations, respectively, and $P_i(\tau_{si})$ the probability of motion of the ith dislocation fraction at the stress τ_{si} and velocity v_i. The normal distribution of the defects over the starting stresses is

$$P_{i}(\tau_{si}) = \int_{\tau_{i-1}}^{\tau_{i}} \frac{1}{\delta\sqrt{2\pi}} \cdot \exp\left[-\frac{(\tau_{si} - \tau_{0}')^{2}}{2\delta^{2}}\right] \mathrm{d}\tau_{si}. \tag{7}$$

The yield stress is

$$\tau_{0}' = \tau_{0} + \alpha\mu b\sqrt{N}, \tag{8}$$

that takes into account the appearance of remote back stresses due to dislocation forest.

2.2. Dislocation density

Expressions of the dislocation density N, the portion of movable defects f and their velocities v_1 can be formed in Appendix A. Taking into account are the Bauschinger's non-ideal effect, generation and deceleration of dislocations.

The total yield stress of the materials under loading takes into account the formation and evolution of the meso-substructures. It is given by

$$\tau_{0}' = \tau_{0} + \alpha\mu b\sqrt{N} + K_{1}'P_{1}(\gamma^{p}) + K_{2}'P_{2}(\gamma^{p}) + K_{3}'P_{3}(\gamma^{p}), \tag{9}$$

where τ_0 is the yield stress of the material before treatment. The model parameters K_j' describe the contributions from the meso-level while $P_j(\gamma^p)$ are the probabilities of the existence of these meso-substructures.

To test the state equations, the stress–strain curves

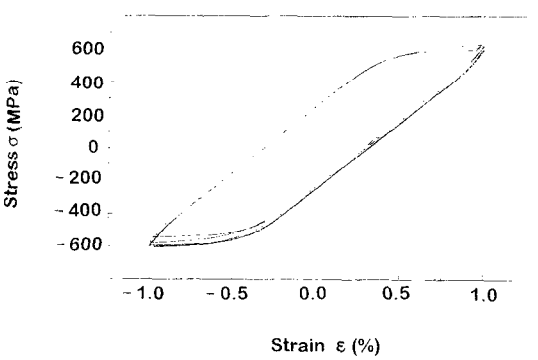

Fig. 2. Calculated stress–strain hysteresis loops for mild steel.

were calculated for the mild steel under cyclic loading ($\dot{\varepsilon}^T = 10^4\ s^{-1}$). The results are presented in Fig. 2. The material constants and parameters of the constitutive equation are given in Refs. [4,5].

3. Results of numerical simulation

3.1. Vibrations

A schematic of ultrasonic wave generation to the specimen is shown in Fig. 1(a). Note that ultrasonic energy can be generated to the specimen either by direct contact with a converter or through a metal concentrator. In this way, sufficient high stresses could be reached to fracture the specimens. The scheme is limited by the resonance length of the system.

The boundary conditions at the output of the specimen used in the numerical calculations can be written as

$$U_1(t) = U_{max} \sin \omega t, \tag{10}$$

where ω is the angular velocity and t the process time. The estimate of the particle velocity amplitude U_{max} is given in Appendix B. The stress value at the free surface of the specimen is equal to zero. High frequency cyclic loading occurs when standing waves are formed in the system that consists of the magneto-strictive converter, concentrator and specimen. In reality, there are some energy redistributions due to assemblage of the components, material inhomogeneity, etc. The actual process lies between the standing and the running waves. Amplitude of the alternative stresses arising from ultrasonic waves is close to the yield stress and extremely sensitive to deviation from the resonance length of the system (see Fig. 3).

Calculations are made for the mild steel specimens subjected to the ultrasonic treatment. They show that accumulation of plastic micro-strains is of a non-linear character and connected with both the evolution of the defect structure on micro-level and the amplitude of the acting macro-stresses. Fig. 4 shows the calculated results for mild steel at different loading stages. Such a character of dislocation accumulation is attributed to the influence of different factors.

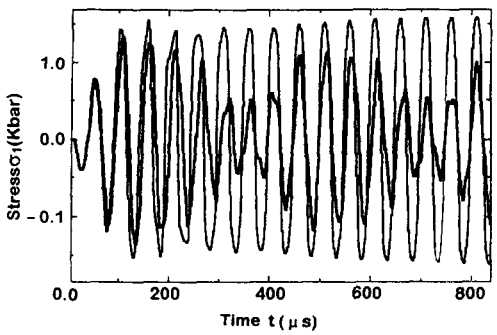

Fig. 3. Calculated stress–time history of mild steel under cyclic ultrasonic loading for different resonance lengths.

Two competing processes are developed simultaneously at micro-level (Fig. 4(a)). On one hand, the alternative stresses generate dislocations, which are then accumulated and moved (plastic flow). On the other hand, the increase of dislocation density leads to development of remote back stresses depressing the dislocation movement (hardening).

Moreover, accumulation of plastic deformations is of highly localized character (Fig. 4(b)). It is caused by standing waves where the most intensive structural evolution occurs in the region away from the nodal stresses. But initiation of the running waves may lead to considerable deviation from symmetric distribution of dislocation density relatively to the center of the specimen.

3.2. Shock waves

The scheme to generate ultrasonic shocks is shown in Fig. 1(b). The deforming tool is pressed to the specimen surface with the constant force F. Ultrasonic vibrations are thus excited in the system. It ensures the high frequency shock treatment. The treatment results in decreasing the surface roughness and cold working layer up to several tens of microns in depth.

The boundary conditions at the converter output is

$$\sigma(t) = \sigma_{const} + \sigma_{max} \sin \omega t, \tag{11}$$

where σ_{const} is the stress due to the static pressing force F, σ_{max} the stress amplitude in the ultrasonic wave, ω the angular velocity of the ultrasonic treatment, and t the process time.

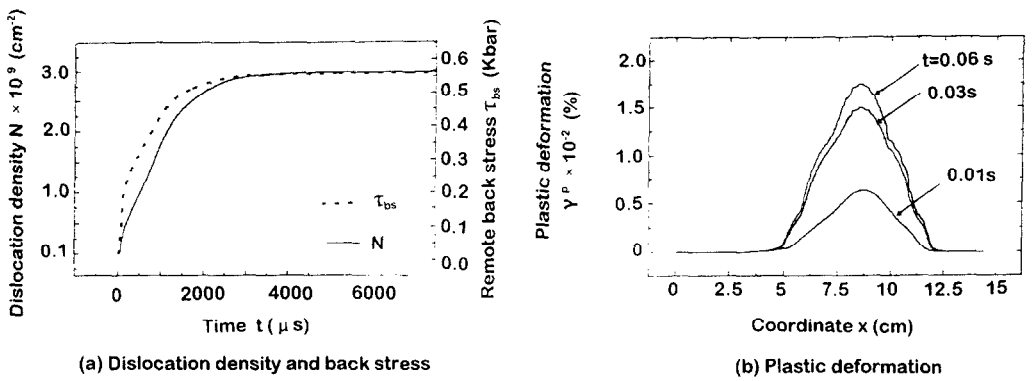

Fig. 4. Cyclic ultrasonic loading with $\xi_m = 20$ μm for (a) dislocation density and remote back stress and (b) plastic deformation.

The motion of the deforming tool depends on the loading parameters and inertial properties of the system. Fig. 5 shows the time-dependence of the deforming tool displacements at the different amplitudes of ultrasonic treatment. The pressing force is 200 N. The calculations show that at lower ultrasonic amplitude (Fig. 5(b)) the frequency of the impacts is higher, but the shock amplitude decreases. The interaction is of complex non-harmonic character with the stress initiating the plastic flow. Accumulation of plastic deformation as quantified in Fig. 6(a) is caused by the evolution of dislocation at the micro-level. This includes the development of meso-sub-structures, fragmentation of the crystals, rotation and displacement of the fragments.

Deforming tools of different shape as well as different amplitudes of pressing and ultrasound are used depending on the desirable effect of tile treatment. For a spherical deforming element, the stress waves propagating into the surface layer are attenuated spherically. The cold worked layer of up to several tens of microns in depth is formed (Fig. 6(b)). The higher the stress amplitude, the deeper the cold worked layer. Usually the time of ultrasonic shock treatment is considerably less than that of pure ultrasonic treatment. It is defined to obtain the maxi-

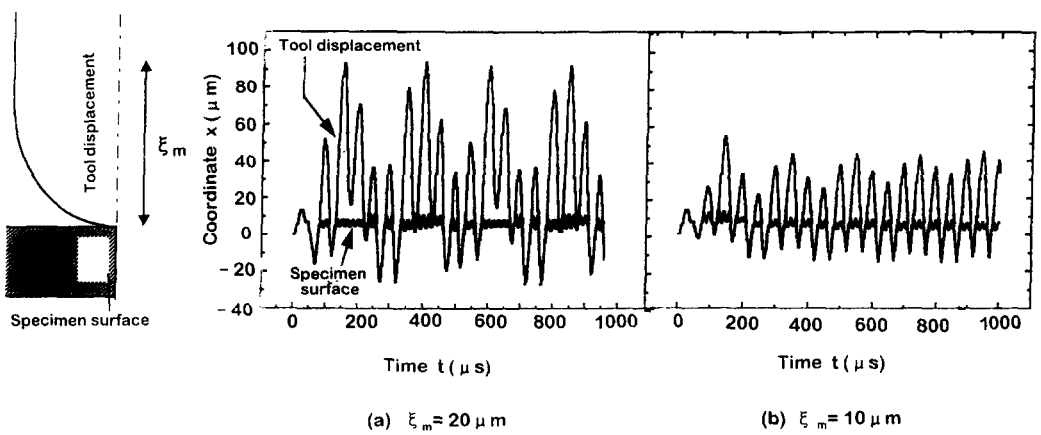

Fig. 5. Ultrasonic shock treatment for different amplitudes: (a) $\xi_m = 20$ μm and (b) $\xi_m = 10$ μm.

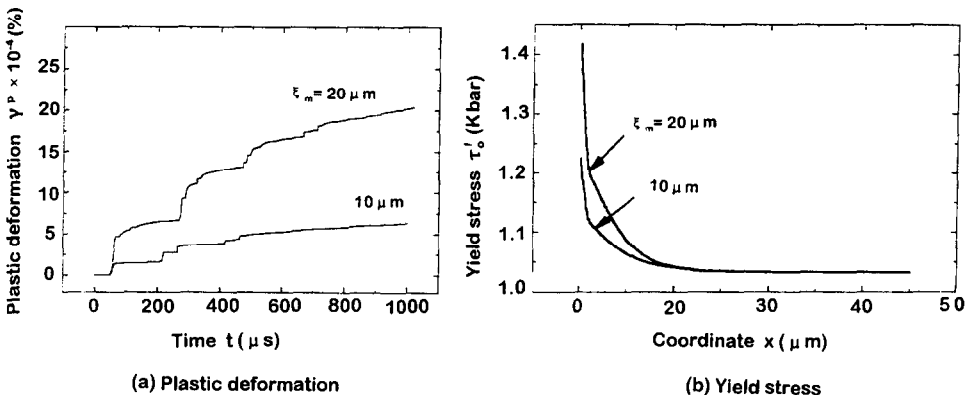

Fig. 6. Ultrasonic shock treatment for different amplitudes: (a) accumulation of plastic deformation and (b) yield stress variations.

mum cold working and to avoid the fracture of the surface.

For ultrasonic polishing, the plane deforming element and small ultrasonic amplitudes are used. In this case, the large contact area and small ultrasound stress amplitude do not cause plastic deformation in the near surface layer and micro-roughness on the surface is only deformed plastically.

4. Conclusion

Presented in this work is the material response of ultrasonic treatment for different amplitudes that could cover a wide range of materials for different methods of coating and surface roughness. A dynamic model is developed whereby predictions could be made to determine the plastic deformation behavior of specimens subjected to different ultrasonic treatments. Results are obtained for mild steel under cyclic or vibratory and shock loading. Agreement between calculated and experimental results is obtained. Accomplished in particular are obtainment of the parameters that would fit the data. They include the oscillation frequency and amplitude, duration of treatment, geometry, etc., in addition to the study of their influence on the deformation process.

Acknowledgements

The work was supported by a grant of Russian Ministry of General and Professional Education for fundamental investigation in the mechanical engineering area.

Appendix A. Dislocation kinetics

In order to determine N, f, and v_1, the empirical expressions suggested in Refs. [4–7] are used. The dislocation density is given by

$$N = N_0 + (N^* - N_0)\exp\left(\frac{A}{|g|b}\gamma_k^p\right), \tag{A.1}$$

where N is initial density of the dislocations. N^* can be interpreted as a limiting dislocation density under loading. The constant A is proportional to the reciprocal of the dislocation free path in the process of multiplication. To take into account plastic strain irreversibility, $\dot{\gamma}^p$ accounts for accumulative plastic deformation:

$$\gamma_k^p = \int_0^t |\dot{\gamma}^p| \mathrm{d}t. \tag{A.2}$$

In an analogous way, the fraction of mobile dislocations is given by

$$f = f^* + (f_0 - f^*)\exp\left(-\frac{B}{|g|b}(\gamma_k^p - \gamma_{kr}^p)\right), \tag{A.3}$$

where f_0 is the initial fraction of mobile dislocations. The quantity f^* can be interpreted as a limiting portion of the mobile defects while the constant B is proportional to the reciprocal of the dislocation

path up to the fixture. To take into account the distinction between resistance to the dislocation travel at the direct and reverse loading, the reverse plastic strain is introduced into Eq. (A.3) such that

$$\gamma_{kr}^{p} = \gamma_{k}^{p}\left(1 - \frac{N}{N^{*}}\right), \tag{A.4}$$

at reversal of the $(\tau - \tau_{bs})$ sign and $\gamma_{kr}^{p} = 0$ in other cases.

The dislocation groups starting to travel under the equal stresses move at the same velocities. These velocities become greater as the difference between τ_{si} and τ increases. They are given by

$$v_i = \begin{cases} v_0 \dfrac{ST_i}{1 + ST_i^2}, & \text{at } |\tau| > \tau_{si}, \\ 0, & \text{at } |\tau| < \tau_{si}. \end{cases} \tag{A.5}$$

Here, v_0 is the acoustic speed and $ST_i = (|\tau| - \tau_{si})/\beta$, with β being the factor of braking.

Appendix B. Pressure and particle velocity amplitude

It has been shown in Ref. [8] that the material displacement in the wave is determined by the harmonic:

$$\xi = \xi_m \sin \omega t, \tag{B.1}$$

where ξ_m is the amplitude of displacement and ω the ultrasonic angular frequency. Hence, the particle velocity is

$$U_1(t) = \xi_t' = \xi_m \omega \cos \omega t. \tag{B.2}$$

The particle velocity amplitude is

$$U_{max} = \xi_m \omega. \tag{B.3}$$

Now, the pressure amplitude may be obtained by the Hugoniout relation:

$$P_{max} = \rho_0 C U_{max}, \tag{B.4}$$

where ρ_0 is the unreformed material density and C the ultrasonic wave velocity.

References

[1] M.L. Wilkins, Calculations of elastic–plastic flow, in: B. Alder. S. Fernbach and M. Rotenberg (Eds.), Methods in Computational Physics, vol. 3, Academic Press, New York, 1964, pp. 211–263.

[2] A.R. Champion, R.W. Rohde, Hugoniot equation of state and the effect of shock stress amplitude and duration on the hardness of hadfield steel, J. Appl. Phys. 41 (5) (1970) 2213–2222.

[3] D.C. Wallace, Equation of state from weak shocks in solids, Phys. Rev. B 22 (4) (1980) 1495–1502.

[4] P.V. Makarov, Mathematical multilevel model of elastic-plastic deformation of heterogeneous structures, Thesis of Physics-Mathematics Science Professor, Tomsk, 1995, 248 pp.

[5] P.V. Makarov, R.R. Balokhonov, V.A. Romanova, V.A. Klimenov, Modelling of accumulation processes of microplastic deformations and damages in meso-volume of metals under ultrasonic loading, Mathematical Method in Physics, Mechanics and Mesomechanics of Fracture, Tomsk, 27–29 Aug., 1996, 63 pp.

[6] J.M. Kelly, P.P. Gillis, Continuum descriptions of dislocations under stress reversals, J. Appl. Phys. 45 (3) (1974) 1091–1096.

[7] J.C. Gilman, Microdynamical theory of plasticity, in: Microplasticity, Metallurgiya Publishers, Moscow, 1972, pp. 18–37.

[8] O.V. Abramov, V.I. Debatnin, V.F. Kazantcev, Power Ultrasonic Action on the Interphase Surface of Metals, Nauka Publishers, Moscow, 1986.